Journal of Engineering Science and Technology
Vol. 13, No. 8 (2018) 2328 - 2341

DESIGN AND ANALYSIS OF OPTICAL SWITCH FOR DATA CENTER NETWORKS INCORPORATING ACO-OFDM WITH PAPR REDUCTION

RAVI KUMAR*, ANURAG TRIPATHI

Dr. Abdul Kalam Technical University, Lucknow, India
Institute of Engineering and Technology, Lucknow, India
*Corresponding Author: raviiitkphd@gmail.com

Abstract

Currently optical data centers heavily rely on electronics for information transfer. In near future electronic switching will face problem in supporting higher data rates. Therefore, a slow migration from electronic to optical switching has been observed. In the notable switch designs, AWG is preferred due to its wavelength routed switching and cyclic nature. However, these devices require expensive TWCs for wavelengths conversions. In data centers, these optical switches can be used to connect racks. To avoid costly TWCs, we can employ OFDM along with AWG for the switching of information. This paper discusses an ACO-OFDM and AWG based optical switch where information from any input can be routed to any output. The problem of PAPR is also discussed and it is suggested that using clipping in addition to μ-Law can reduced PAPR significantly.

Keywords: ACO-OFDM, AWG, Optical switching, PAPR, TWC.

1. Introduction

The design of optical switch in data-centers is an important and hot area of research. In optical data, center networks at many places switches are used to connect various level of hierarchy. The optical switches can be placed in data center networks where switching of information is necessary. Moreover, in data centers data rate is different at various switching positions. Therefore, at different positions optical switches device can be different. The lowest data rates switches are at the bottom of the hierarchy, which are used to connect ToR to ToR connections (Fig. 1).

In recent past, many designs for data-centers have been proposed including buffer-less and buffered designs [1-5]. In buffered designs electronic, optical and hybrid, buffers are considered [6]. Buffered designs are more complex while buffer-less design are relatively simple [1, 6]. However, buffer designs have better packet loss performance [7].

Recently O-OFDM is considered as excellent way of transmission for optical signal. However, O-OFDM only supports relatively low data rates. Therefore, O-OFDM based switches can be used to establish ToR to ToR connections.

In typical (non-optical) OFDM systems, the information is transferred using bi-polar electrical field signals. For the coherent receiving, a local oscillator along with low pass filter is used. However, in optical communication intensity of laser is used for information transfer, which is a positive signal (Uni-polar). On the receiver, side direct detection is used.

The use of O-OFDM in the field of optical data centre design is a novel area of research. In these designs, both optical and electrical parameters need to be considered as design parameters. Moreover, design parameters of O-OFDM also need to be investigated.

Most of recently proposed designs are based on cyclic AWG router, which is a wavelength sensitive routing device, and it is capable of handling multiple wavelengths simultaneously. As AWG is a cyclic device therefore for non-blocking operation of AWG only a few wavelengths are needed (Fig. 2). In past various AWG based design, like buffer-less, feed-forward type buffer, feed backward type buffer, re-circulating type buffer are common. In data, centers where hundreds of such switches would be needed demands for less complex cost effective design. An AWG is an excellent device as each input is connected to each output via a fixed wavelength, therefore using AWG, one to one and many to one connections are possible [7, 8]. Moreover mesh connections where all inputs and outputs are connected is also possible as shown in Fig. 2.

In recently proposed design, TWC and AWG based are used to connect ToR switches as shown in Fig. 3 [5]. First of label extractor (LE) is used to extract the label it is processed by controller and as per the information TWC wavelength is selected either for straight path or to put packet inside the buffer. Here in this design buffer is assumed to be electronic in nature, thus information is stored through O/E conversion and retrieved by E/O conversion again. From here information can be send to correct output by tuning its wavelength through buffer TWC. In this design in a single time slot, only one input connects to one output only and only one packet will exit the buffer in a single time slot. Moreover, TWC technology is not fully matured and currently available TWCs are noisy in nature.

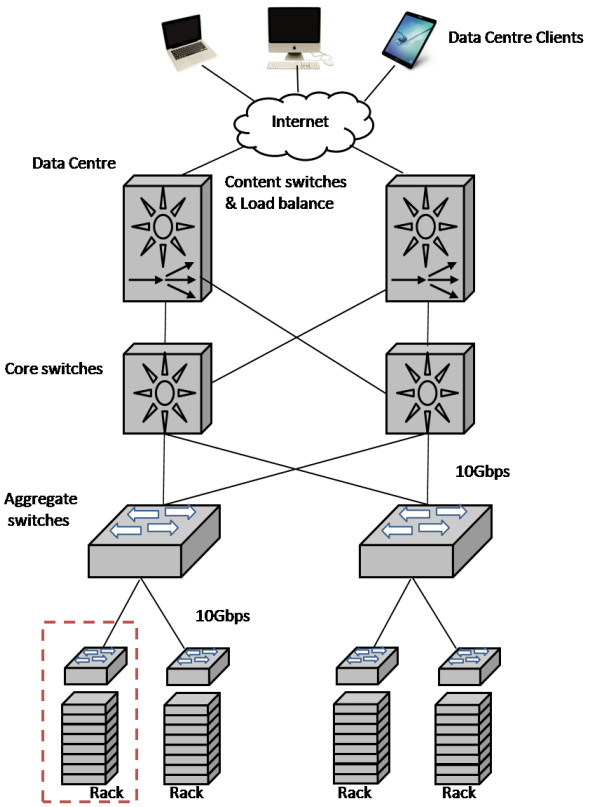

Fig. 1. Schematic of data center networks.

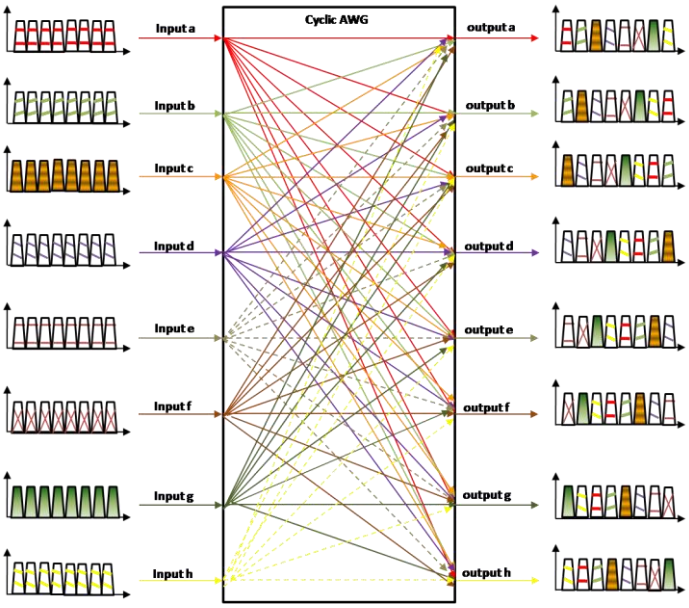

Fig. 2. Schematic of cyclic arrayed waveguide optical router.

To overcome these problems in this paper we have discussed an OFDM and AWG based switch, which is non-blocking in nature, thus no need of buffer in such arrangement.

This paper discusses AWG based switch design for data centers application using OFDM technology. First of all physical layer analysis is performed. It is discussed that how ACO-OFDM can be used in data centers. Finally, a hybrid method is suggested to reduce PAPR significantly.

The rest of the paper is organized as follows: in section 2 of the paper, MIMO OFDM in data centre networks is discussed. MIMO-OFDM cyclic optical router is detailed in section 3 of the paper. In section 4 of the paper BER analysis is performed. In section 5 of the paper ACO-OFDM is discussed, and in section 6 PAPR mitigation techniques are discussed ad finally section 7 of the paper discusses major conclusions.

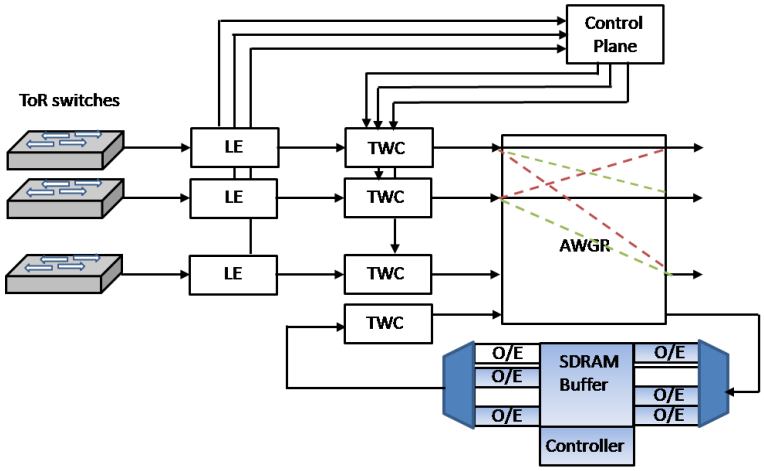

Fig. 3. Schematic of optical router based on TWC and AWG.

2. MIMO OFDM in Data Centre Networks

In the case of an OFDM transmitter, serial data streams are collected and mapped into N_C constellation symbols $\{\{S[k]\}_{k=0}^{N_c-1}\}$ by making use of BPSK or QPSK N_p pilots are embedded into the data symbols prior to transforming into the time domain signal by N-orthogonal subcarriers through an IFFT given as

$$s(n)=\frac{1}{\sqrt{N}}\sum_{k=0}^{N-1}S[k]e^{\frac{j2\pi nk}{N}}, \quad n=0,1,...,N-1 \tag{1}$$

At every receiver, a typical photo-detector (PD) receives O-OFDM signals from various input sources on different optical wavelengths, with no conflict in the OFDM subcarriers and the used WDM wavelengths. This is known as parallel signal detection (PSD) technique [9], and this technique has been shown in OFDM WDM-based optical networks [9].

In optical transmission, we have two kinds of OFDM execution. The first kind is of the electrically creation of the OFDM signal and modulation of the signal to

an optical carrier [10-12]. This kind of execution is termed as optical OFDM (OOFDM). There is an option for the receiver to make use of either direct detection or coherent detection strategies. The next kind is to develop the orthogonal subcarriers (otherwise known as tones) optically and after that make an application of a signal onto each subcarrier [12]. This is known as the all-optical OFDM (AO-OFDM).

3. Mimo-OFDM Cyclic Arrayed Waveguide Optical Router

The ToR switches may require to connect with severs or switches in these connections; a low bit rate link is desirable which can be achieved using MIMO OFDM system as shown in Fig. 4. The ACO-OFDM based switch consists of N racks, which are connected by ToR switch. Each of the rack contains multiple servers. The communication among different ToR is accomplished using DCN.

The signals from different racks are combined at each rack and send to a transmitter consisting OFDM modulator, which converts the aggregated information to j subcarriers and these subcarriers, are converted into j WDM signals using DML. It is noticeable that $0 \leq j \leq N$. These WDM signals are detected by PDs at each output port of AWG and after OFDM demodulation process directed towards output ToR. It is noticeable that each photo-detector can detect multiple signals using PSD technology. In this technology, more than one signal can be detected simultaneously using array of detectors.

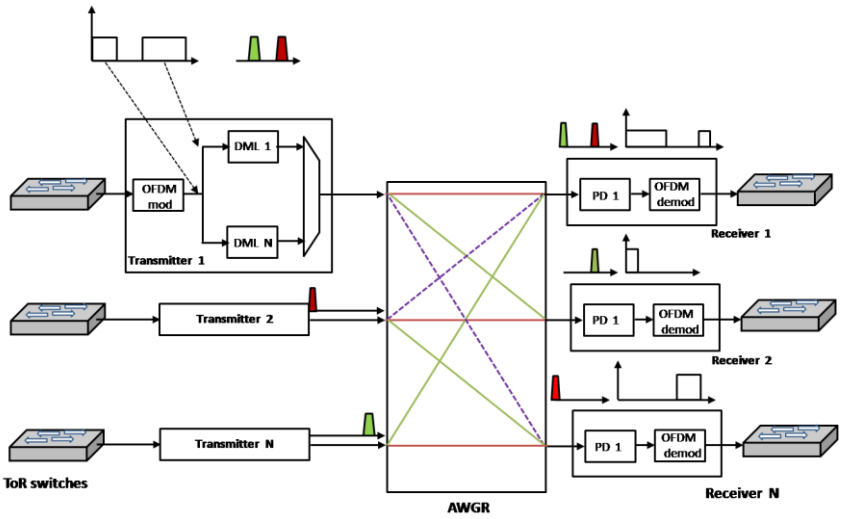

Fig. 4. Schematic of MIMO- OFDM cyclic arrayed waveguide optical router.

The DCN design depends on an O-OFDM execution. It shows network level MIMO operation in light of the fact that all racks are able to transmit the similar OFDM signal to various goal racks at the same time, and numerous racks are able to transfer the signal to the same particular rack in the meantime by modulating data on various OFDM subcarriers. In DCN, distance between the ToR switches is in the

range of a few tens of meters to 2 km [4]. Therefore, fiber optic degradation like pulse broadening, jitter, and polarization mode dispersion will not come into picture.

4. BER Analysis

In this design from DML to PDs signal propagates in optical domain. The power budget analysis is essential to know about the minimum power requirement for the correct operation of the switch. The loss in signal power when packet directly passes through the switch is

$$A_L = L_{DML} L_{MUX} L_{AWG} \tag{2}$$

Thus power available at the output of the optical switch is

$$P_{out}(b) = A_L b P_{in} \qquad b \in [0,1] \tag{3}$$

At the receiver, both shot and thermal noises are present, and for the bit {b ε (0, 1)} the noises at the optical receiver are [13, 14]:

Shot noise: $\sigma_s^2 = 2qRPB_e$ and thermal noise: $\sigma_{th}^2 = \dfrac{4K_B T B_e}{R_L}$

The total noise variance is

$$\sigma^2(b) = \sigma_s^2 + \sigma_{th}^2 \tag{4}$$

The Bit Error Rate (BER) can be obtained as

$$BER = Q\left(\frac{I(1)-I(0)}{\sigma(1)+\sigma(0)}\right) = Q\left(R\frac{P(1)-P(0)}{\sigma(1)+\sigma(0)}\right) \tag{5}$$

where $Q(.)$ is error function and defined as

$$Q(z) = \frac{1}{\sqrt{2\pi}} \int_z^{\infty} e^{-\frac{z^2}{2}} dz \quad . \tag{6}$$

Using the above formulations and value of different parameters as given in Table 1, results are shown in Figs. 5 and 6.

Table 1. List of parameters and their values.

Parameters	Value
Electronic Charge	1.6×10^{-19} C
Responsivity	1.28 A/W
Electrical bandwidth	20 GHz
Optical bandwidth	40 GHz
Loss of AWG (32 channels)	3.0 dB
Loss of DML	1 dB
Loss of MUX	3.0 dB
Boltzmann Constant	1.38×10^{-23} m^2 kg s^{-2} K^{-1}
Load Resistance	50 Ω
Planck Constant	6.6×10^{-34} J-s

In Fig. 5, BER vs. optical and electrical powers is shown. Here, received power is 7 dB below to the transmitted power. BER of ~10^{-9} is obtained for received

power of -17.46 dBm, thus corresponding transmitted power is -10.46 dBm. For slight increase in power to -17dBm, the obtained BER~10^{-12}. For BER of ~10^{-9} the OSNR (optical signal to noise ratio) is 7.9 dB and ESNR (electrical signal to noise ratio) is 15.8 dB.

In single carrier system, information is transmitted in form of bits using single carrier only, while in multi-carrier system, more than one carrier are used for information transfer. OFDM is also a multi-carrier transmission technology, where multiple carriers known as sub-carrier used for information transfer. However, in OFDM each sub-carrier carries data from a common source only. Due to the multiple carries inclusion via IFFT, OFDM signal in time domain have high peak-to-average power ratio (PAPR)

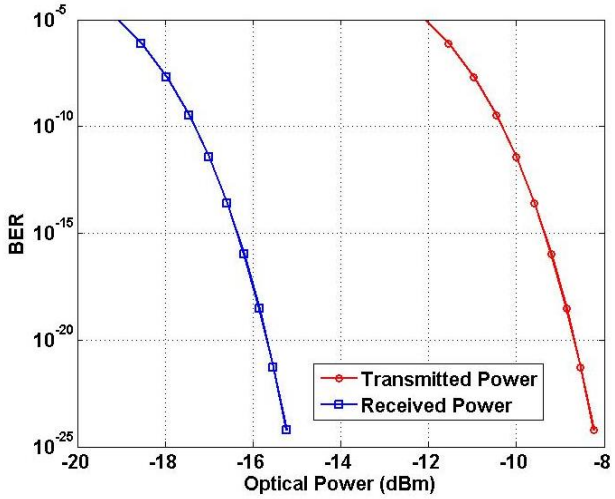

Fig. 5. BER vs. optical transmitted and received powers.

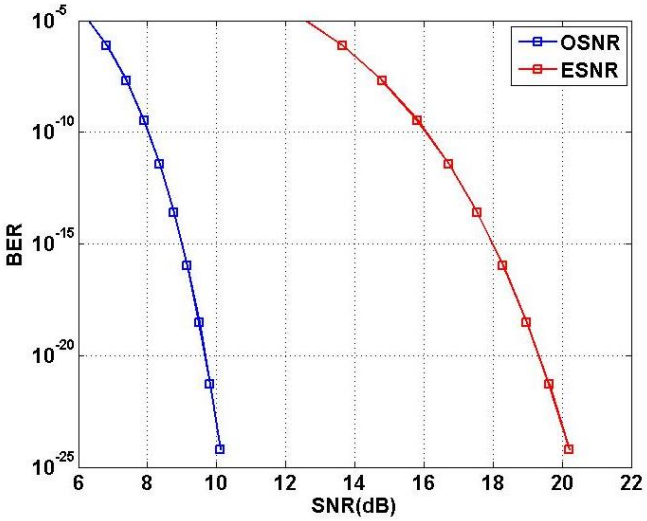

Fig. 6. BER vs. optical and electrical SNR.

In optical communication, two variants of OFDM namely DC-biased optical OFDM (DCO-OFDM) and asymmetrically clipped OFDM (ACO-OFDM) are used. Both these techniques satisfy Hermitian symmetry. In DCO-OFDM all the sub-carriers carries information while in ACO-OFDM only odd subcarriers carry information. In DCO-OFDM to clip negative part DC biased is added which lead to distortion and in-efficient detection system. Therefore, in this work ACO-OFDM is used.

5. ACO-OFDM

The ACO-OFDM system transmitter is shown by the Fig. 7 [12]. Data symbols are carried by the only the odd subcarriers in ACO-OFDM, while as far as the even subcarriers are concerned, they are set to zero, i.e., $S_k = 0$ for $k = 0, 2, 4,..., N\text{-}2$. Meanwhile, ACO-OFDM additionally fulfils the Hermitian symmetry, i.e., $S_k = S_{N-k}$ in the frequency domain and consequently contains the accompanying frame structure.

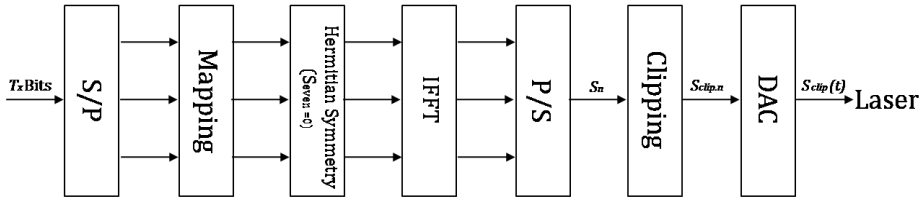

Fig. 7. Block diagram of aco-ofdm transmitter mechanisms.

$$S = \left[0, S_1, 0, ...S_{\frac{N}{2}-1}, ...0, S_1^* \right]. \tag{7}$$

After the IFFT, we have the time-domain signal for $n = 0,..., N - 1$

$$s_n = \frac{1}{\sqrt{N}} \sum_{k=0}^{N-1} S_k e^{j\frac{2\pi kn}{N}} = \frac{2}{\sqrt{N}} \sum_{k=1}^{\frac{N}{2}-1} \mathrm{Re}\left\{ S_k e^{j\frac{2\pi kn}{N}} \right\} = \frac{2}{\sqrt{N}} \sum_{t=1}^{N/4} \mathrm{Re}\left\{ S_{2t-1} e^{j\frac{2\pi(2t-1)n}{N}} \right\}$$

It must be noted here that the time-domain signal of ACO-OFDM has accompanying symmetric property:

$$s_{n+\frac{N}{2}} = \frac{2}{\sqrt{N}} \sum_{t=1}^{N/4} \mathrm{Re}\left\{ S_{2t-1} . e^{j\frac{2\pi(2t-1)\left(n+\frac{N}{2}\right)}{N}} \right\} = -s_n, \quad n = 0,....., \frac{N}{2} - 1 \cdot \tag{8}$$

Consequently, it is clear that anyone can make the transmission of the positive part of s_n and can also clip its negative part without making any sort of change in information. We can represent this kind of clipping process along with the upper bound limit as

$$s_n^c = \text{Clip}[s_n] = \begin{cases} c_u, & s_n \geq c_u \\ s_n, & 0 < s_n < c_u \\ 0, & s_n \leq 0 \end{cases} \tag{9}$$

Due to the fact that s_n^c is nonnegative, we do not require to make addition of a DC bias. After this, we convert the clipped signal into the continuous signal $s^c(t)$ for making the transmission through a laser.

In Fig.8, BER analysis of ACO-OFDM under QPSK and 8-PSK modulation schemes is shown. Here the BER performance of QPSK scheme is much better in comparison to 8-PSK. Still under both the schemes at low ESNR very low BER is possible. Therefore, to meet BER criterion for OFDM part and optical part a proper transmitted power should be selected for both analog and optical transmission.

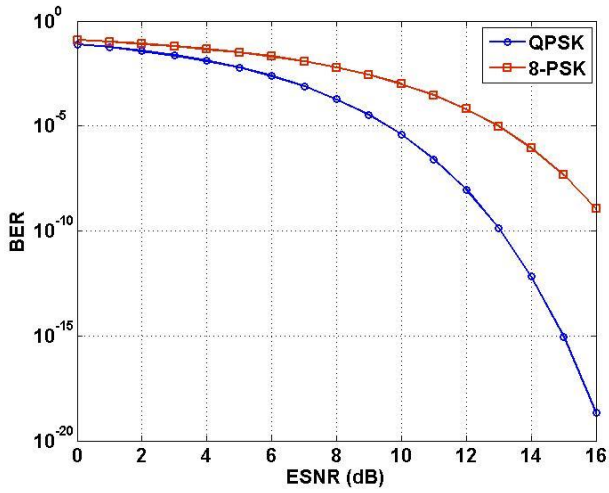

Fig. 8. BER analysis of ACO-OFDM under QPSK and 8-PSK modulation schemes.

In OFDM systems, PAPR is other important issue, which should be addressed. PAPR is calculated as ratio of maximum power of a signal to its average power [15]:

$$PAPR = \frac{\max\left(|s_n|^2\right)}{E\left(|s_n|^2\right)}. \tag{10}$$

where *E* denotes expected value. In case of large number of sub-carriers this is a common phenomenon and cannot be avoided. However, to mitigate such detrimental effect a few schemes are proposed as discussed in next section.

6. PAPR Mitigating Techniques

In this Section, various PAPR mitigation techniques are discussed. These techniques have been modified in the paper to meet ACO-OFDM requirements and optical communication.

6.1. Clipping and filtering

Generally, clipping is performed at the transmitter side. In this method, amplitudes of the bins, which are above than pre-defined threshold are, clipped (Fig. 9). This clipping reduces the variability in the amplitudes for PAPR reduces. However, clipping of signals introduces both in band distortion and out of band radiation into OFDM signals, thus BER performance also degrades.

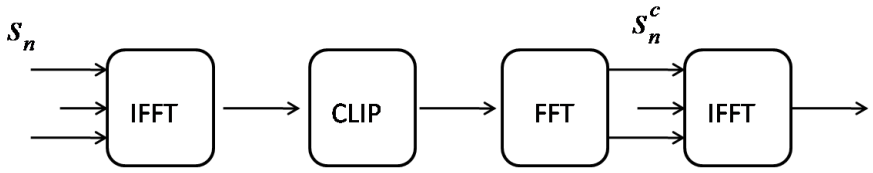

Fig. 9. Block diagram of clipping.

Filters are used to cut out of band radiation after clipping however; it cannot reduce in-band distortion. However, due to clipping and filtering some peak may re-growth. This can be understood as

$$y[n] = \sum_{k=0}^{LN} x[k]h[n-k] \tag{11}$$

where $y[n]$ is output after filtration process, $x[n]$ is OFDM symbol, $h[n]$ is filter response, L is channel length and N is number of OFDM symbols. Due to the convolution sum, the amplitude value increases. In the considered design (Fig. 4), AWG itself is a wavelength sensitive device, thus, it will eliminate out of band noise without affecting the amplitude levels of inband symbols. Thus in OOFDM the dis-advantage of filter removed completely.

6.2. μ-Law Mapping

Companding techniques are no-linear techniques, which reduces the variability in the amplitudes of the bins [16]. In the companding techniques bins whose amplitudes are smaller get amplified however, if amplitude is higher than certain threshold it remains nearly same. Thus, variability in the amplitude gets reduced.

In the μ-law companding, signal is squeezed at the transmitter considering formula:

$$s_n^{'} = \frac{\max(s_n)\ln\left(1+\dfrac{\mu|s_n|}{\max(s_n)}\right)}{\ln(1+\mu)} \tag{12}$$

where μ is the μ-law compression parameter. At the receiver site μ-law signal is expands as:

$$s_n = \frac{\max(s_n)}{\mu}\left(e^{|s_n^{'}|\frac{\ln(1+\mu)}{\max(s_n)}} - 1\right) \tag{13}$$

Figure 10 demonstrates the μ-OFDM system building blocks. We can differentiate O-OFDM and RF-OFDM in the way of signal transmission. In O-OFDM real and imaginary parts are separated and only positive signals are

transmitted. After this, μ-law mapping is performed. Now at this point, E/O conversion data is converted into optical domain and transmitted. Than signal is passed through optical channel, and inverse process is repeated at the receiver.

In this work, we have proposed a hybrid scheme where both μ-law companding scheme and clipping based scheme is proposed where filtering action will be performed by AWG.

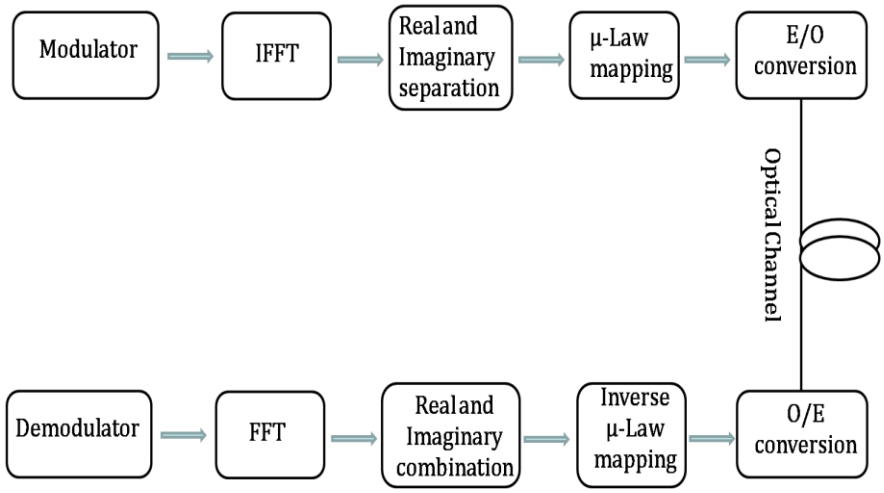

Fig. 10. μ-law based optical OFDM system.

In Fig. 11(a), normal ACO-OFDM signal plot in terms of amplitude vs. bin is shown. Here bin represents index value. In figure, a large variation in amplitude is observed. The maximum observed value is 0.0537 and minimum observed value is 6.5×10^{-4}. To tackle this large variation clipping is used and observed results are shown in Fig. 11(b). Here, if particular bin value is higher than 0.7×maximum amplitude value than it is bring down to 0.7×maximum amplitude value, thus bin values above this are clipped. Now the maximum value is 0.0376.

In Fig. 11(c) μ-law based ACO-OFDM signal plot in terms of amplitude vs. bin is shown, with maximum amplitude as 0.0805 and minimum value as 0.0405. However, using μ-law the variation in amplitude gas reduced significantly. In Fig. 11(d) μ-law, clipped and ACO-OFDM signal plot in terms of amplitude vs. bin is shown. Here, in comparison to Fig. 11(a), the variation in amplitude has reduced significantly, and after inversing mu-law original signal can be recovered.

It is clear from Figs. 12 that as bin size reaches to a value of 1000, PAPR values stabilizes. The PAPR of generated ACO-OFDM is nearly 26 dB, which reduces to 19 dB with clipping. While using mu-law, PAPR reduces to nearly 5 dB, which now with clipping reduces to 1.3 dB. This reduction in PAPR is possible due to the AWG, which works as filter, and additional filter is not needed after clipping. Therefore, amplitude is stabilized and multi-stage clipping and filtering is not required as in case of separate filtering amplitude of the signal increases due to convolution effect.

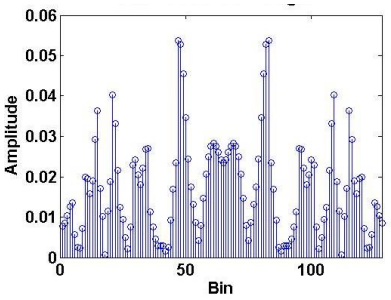

(a) ACO-OFDM signal plot in terms of amplitude vs. bin.

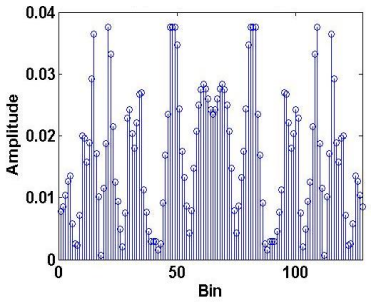

(b) Clipped ACO-OFDM signal.

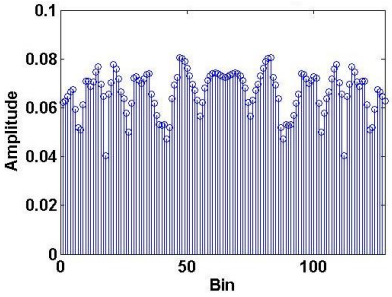

(c) μ-law based OOFDM signal plot in terms of amplitude vs. bin

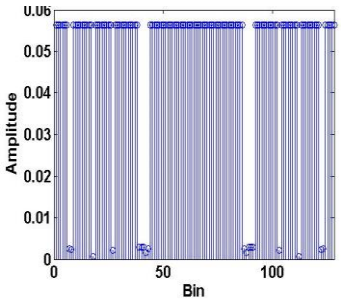

(d) μ-law and clipped based OOFDM signal plot.

Fig. 11. Performance of ACO-OFDM under different scenarios.

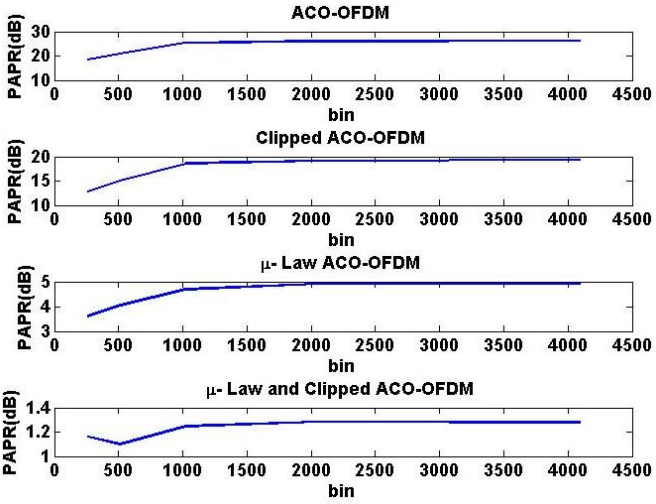

Fig. 12. Comparison of PAPR reduction techniques.

7. Conclusions

This paper presents an analysis of optical switch design for DCN, which is based on MIMO-OFDM technology. The considered design provides error free and non-

blocking performance among ToR switches. To meet optical requirements ACO-OFDM is considered. BER performance for both optical and ACO-OFDM is evaluated. The problem of PAPR is also highlighted, and solutions are suggested to improve the performance. Simulation study is performed to obtain PAPR under different schemes. It has been found that the proposed scheme is much superior in comparison to other considered schemes.

Nomenclatures

A_L	Total Loss
b	Bit
B_e	Electrical Bandwidth
I	Photo-current
L_{Twc}	Loss of TWC, dB
L_{MUX}	Loss of Multiplexer dB
L_{AWG}	Loss of Arrayed Waveguide Gratings, dB
N	Number of sub-carriers
q	Electronic Charge
Q	Error Function
S	Sub-carrier
T	Temperature
K_B	Boltzmann Constant
R_L	Load Resistance

Greek Symbols

σ^2	Variance
μ	Constant

Abbreviations

ACO-OFDM	Asymmetric Clipped Optical Orthogonal Frequency Division Multiplexing
AWG	Arrayed Waveguide Gratings
BER	Bit Error Rate
BPSK	Binary Phase Shift Keying
DC	Direct Current
DCN	Data Centre Networks
DML	Direct Modulated Laser
EDFA	Erbium Doped Fiber Amplifier
IFFT	Inverse Fast Fourier Transform
LE	Label Extractor
MIMO	Multiple Input Multiple Output
OFDM	Orthogonal Frequency Division Multiplexing
PAPR	Peak to Average Power Ratio
PD	Photo-detector
PSD	Parallel Signal Detection
QPSK	Quadrature Phase Shift Keying
ToR	Top of Rack
TWC	Tunable Wavelength Convertor
WDM	Wavelength Division Multiplexing

References

1. Ye, X.; Yin, Y.; Yoo, S.B.; Mejia, P.; Proietti, R.; and Akella, V. (2010). DOS: A scalable optical switch for datacenters. *Proceedings of the 6th ACM/IEEE Symposium on Architectures for Networking and Communications Systems*, La Jolla, CA, USA
2. Shukla, V.; Jain, A.; and Srivastava, R. (2016). Design of an arrayed waveguide gratings based optical packet switch. *Journal of Engineering Science and Technology* (*JESTEC*), 11(12), 1705-1721.
3. Shukla, V.; Jain, A.; and Srivastava, R. (2016). Performance evaluation of an AWG based optical router. *Optical and Quantum Electronics*, 48(1), 69.
4. Yin, Y.; Proietti, R.; Nitta, C.J.; Akella, V.; Mineo, C.; and Yoo, S.J.B. (2013). AWGR-based all-to-all optical interconnects using limited number of wavelengths. *Proceedings of the 2003 Optical Interconnects Conference*, 47-48.
5. Yin, Y.; Proietti, R.; Ye, X.; Nitta, C. J.; Akella, V.; and Yoo, S. J. B. (2013) LIONS: An AWGR-based low-latency optical switch for high performance computing and data centers. *Journal of Selected Topics in Quantum Electronics* 19(2), 3600409-3600409.
6. Wang, J.; McArdle, C.; and Barry, L.P. (2016). Optical packet switch with energy-efficient hybrid optical/electronic buffering for data center and HPC networks. *Photonic Network Communications*, 32(1), 89-103.
7. Rastegarfar, H.; Leon-Garcia, A.; LaRochelle, S.; and Rusch, L.A. (2013). Cross-layer performance analysis of recirculation buffers for optical data centers. *Journal of Lightwave Technology*, 31(3), 432-445.
8. Srivastava, R.; and Singh, Y. N. (2010). Feedback fiber delay lines and AWG based optical packet switch architecture. *Journal of Optical Switching and Networking*, 7(2), 75-84.
9. Luo, Y.; Yu, J.; Hu, J.; Xu, L.; Ji, P. N.; Wang, T.; and Cvijetic, M. (2007). WDM passive optical network with parallel signal detection for video and data delivery. *Optical Fiber Communication and the National Fiber Optic Engineers Conference, 2007. OFC/NFOEC 2007*, 1-3.
10. Lowery, A.; Du, L.; and Armstrong, J. (2007). Performance of optical OFDM in ultralong-haul WDM lightwave systems. *Journal of Lightwave Technology*, 25(1), 131-138.
11. Shieh, W.; Bao, H.; and Tang, Y. (2008). Coherent optical OFDM: Theory and design. *Optics Express*, 16(2), 841-859.
12. Dissanayake S.D.; and Armstrong J. (2013). Comparison of ACO-OFDM, DCO-OFDM and ADO-OFDM in IM/DD systems. *Journal of Lightwave Technology*, 31(7), 1063-1072.
13. Srivastava, R.; Singh, R.K.; and Singh, Y.N. (2009). Design analysis of optical loop memory. *Journal of Lightwave Technology*, 27(21), 4821-4831.
14. Olsson, N. A. (1990). Lightwave system with optical amplifiers. *Journal of Lightwave Technology*,7(7), 1071-1082.
15. Popoola, W.O.; Ghassemlooy, Z., and Stewart, B.G. (2014). Pilot-assisted PAPR reduction technique for optical OFDM communication systems. *Journal of Lightwave Technology*, 32(7), 1374-1382.
16. Hasan, M.M. (2014). A new PAPR reduction scheme for OFDM systems based on gamma correction. *Circuits, Systems, and Signal Processing*, 33(5), 1655-1668.